Published in final edited form as:
Biochem J. 2013 January 15; 449(2): 491–496. doi:10.1042/BJ20121155.

Investigations on the Oxygen Dependence of a 2-Oxoglutarate Histone Demethylase

Elena M. Sánchez-Fernández, **Hanna Tarhonskaya**, **Khalid Al-Qahtani**, **Richard J. Hopkinson**, **James S. O. McCullagh**, **Christopher J. Schofield**, and **Emily Flashman***
Chemistry Research Laboratory, University of Oxford, 12 Mansfield Road, Oxford, OX1 3TA, United Kingdom

SYNOPSIS

Histone N^{ε}-methyl lysine demethylases are important in epigenetic regulation. KDM4E is a representative member of the large Fe(II)/2-oxoglutarate dependent family of human histone demethylases. We report kinetic studies on the reaction of KDM4E with O_2: Steady-state assays show KDM4E has a graded response to O_2 over a physiologically relevant range of O_2 concentrations. Pre-steady state assays imply that KDM4E reacts slowly with O_2 and that there are variations in reaction kinetics dependent on the methylation status of the substrate. The results demonstrate the potential for histone demethylase activity to be regulated by oxygen availability.

Keywords

histone demethylases; KDM4E; oxygen; kinetics; stopped-flow spectroscopy

INTRODUCTION

Post-translational modifications to histone tails enable the dynamic regulation of transcription, and are important in development and differentiation and in diseases including cancer [1,2]. N^{ε}-Lysine histone methylation can be transcriptionally activating or deactivating depending on the target residue and its methylation status [3]. Two classes of histone demethylase have been identified, the largest of which uses O_2 and 2-oxoglutarate (2OG) as cosubstrates. The Fe(II) and 2OG dependent KDM4 (JMJD2) histone demethylases (JmjC enzymes) are selective for tri- and di-methylated lysines at H3K9 (histone H3 lysine9) and/or H3K36. Like other JmjC enzymes, human KDM4E, which acts on H3K9 (Figure 1), has the structural features typical of Fe(II)/2OG oxygenases, namely a core double stranded beta helix fold and an Fe(II) binding triad of HXD/E…H residues [4] (Supplementary Figure S1). The proposed mechanism for the 2OG dependent KDMs is based on the consensus mechanism for the 2OG oxygenases. It is proposed that O_2 binds to the KDM4E:Fe(II):2OG:H3K9 complex (I-III, Figure 1) with subsequent formation of a

*Corresponding Author: emily.flashman@chem.ox.ac.uk, Telephone: +44 (0)1865 285110, Fax: +44 (0)1865 285002.

Author Contributions

Elena M. Sanchez-Fernandez conducted the majority of the experiments, analysed data and wrote the paper. Hanna Tarhonskaya conducted the steady state oxygen assays, analysed data and wrote the paper. Khalid Al-Qahtani conducted the LC/MS experiments and James McCullagh contributed to MS analysis. Richard Hopkinson conducted the NMR experiments. Christopher Schofield and Emily Flashman designed the study and wrote the paper.

Europe PMC Funders Author Manuscripts

reactive Fe(IV)-oxo species that performs hydroxylation of the substrate C-H bond (IV-VI, Figure 1). The hydroxymethyl product is released as HCHO (VII, Figure 1) giving the *N*-demethylated product [4-6]. Aspects of the consensus mechanism for 2OG oxygenases are supported by a body of kinetic, structural and spectroscopic evidence on different enzymes [5].

Studies on the Fe(II)/2OG-dependent bacterial taurine dioxygenase (TauD) and viral prolyl-4-hydroxylase (vCPH) [6,7] support the rapid formation (< 1s) of an Fe(IV)-oxo species after O_2 binding. In contrast, studies on the Fe(II)/2OG oxygenase human prolyl hydroxylase domain isoform 2 (PHD2), a hypoxia-inducible factor (HIF) hydroxylase with a proposed O_2-sensing role, reveals that under similar conditions PHD2 does not react rapidly with O_2 [8]. PHD catalysed hydroxylation was observed to be ~100-fold slower than for TauD, a property that could be related to its role as an O_2 sensor [8].

Given that histone methylation status plays an important role in the regulation of transcription, that hypoxia can have epigenetic consequences [9], and that some 2OG oxygenases play roles in hypoxic sensing, it seems possible that KDM catalysis is regulated by O_2 availability. It is reported that histone methylation status can be affected by hypoxia [10] and some KDMs, including KDM4E, mutations to which are linked to cancer, are regulated by HIF/hypoxia [11]. The work with PHD2 raises the possibility that a hallmark of an O_2 sensing oxygenase may be slow reaction with O_2. The kinetics of the reaction of KDMs with O_2 are thus of biochemical interest and potential physiological relevance. We have therefore carried out kinetic investigations on the reaction of KDM4E with respect to O_2. Although KDM4E is encoded for by a putative pseudogene [12,13], it is suited to kinetic analyses. We report studies on the O_2-dependence of KDM4E. The results show that KDM4E activity varies over a physiologically relevant range of O_2 concentrations, and in pre-steady state experiments is apparently slow to react with O_2, in comparison with TauD and vCPH [6,7], and is more similar to PHD2 [8]. Notably the rate of formation of apparent intermediates is dependent on the methylation state of the substrate.

MATERIALS AND METHODS

Preparation of the Histone Demethylase, KDM4E, and Substrates

The catalytic domain of human KDM4E (residues 1-337) was produced as an *N*-terminally His_6-tagged protein in *Escherichia coli*, purified by Ni-affinity and size-exclusion chromatography, and stored at a concentration of 60 mg mL^{-1} in 50 mM Hepes/500 mM NaCl, pH 7.5 [14].

Synthesis of peptide substrates was carried out using standard Fmoc-based solid phase peptide synthesis (SPPS) with a CSPep336X peptide synthesiser (CSBio, California, USA). Peptides were synthesised on a PL-AMS (aminomethylpolystyrene) resin (Polymer Labs) by using a Rink amide linker, cleaved from the resin using trifluoroacetic acid/ triisopropylsilane (97.5/2.5) and purified by reverse phase HPLC on a C18-silica column prior to use. Sequence of the H3K9 8mer peptides: ARK(me0/me1/me2/me3)STGGK. Sequence of the H3K9me3 25mer peptide: ARTKQTARKme3STGGKAPRKQLATKVA. Peptide mass was confirmed by MALDI-TOF-MS spectrometry.

Steady-state KDM4E assay at varying oxygen concentrations

Steady-state studies of KDM4E O_2 dependence were performed in an "In vivo hypoxia workstation 500" (Ruskinn) at 37 °C varying O_2 content from 0.5 to 20.6%. Initial rates of the enzymatic reaction were determined by preparing an assay mix in 50 mM Hepes, pH 7.5, pre-equilibrated in the hypoxic workstation, containing KDM4E (1 μM), H3K9me3/H3K9me2 peptide (100 μM), 2OG (100 μM), NH_4FeSO_4 (10 μM) and L-ascorbic acid (100 μM). To stop the reaction after defined time points, assay solutions (1 μL) were spotted onto the target plate and mixed with α-cyano-4-hydroxycinnamic acid (CHCA) MALDI matrix (1 μL) and allowed to dry before analysis. Samples were analyzed using a Waters Micromass™ MALDI microMX™ mass spectrometer in positive ion reflectron mode with flight tube voltage at 12 kV and reflectron voltage at 5.2 kV. Data were analysed using MassLynx™ version 4.0. Ion counts for methylated and demethylated peptide as a fraction of the total peptide ion count were used to calculate demethylation ratios (Equation 1 in the SI). All assays were performed at least in triplicate.

UV-Visible Absorption Spectroscopic Experiments

Absorption spectra were acquired using a Cary Varian 4000 UV-Vis spectrophotometer at room temperature with 0.4 mM KDM4E and 4.0 mM 2OG in deoxygenated 50 mM Hepes/500 mM NaCl, pH 7.5, followed by titration with Fe(II) in an anaerobic glove box leading to formation of KDM4E:2OG:Fe(II) complex. The sample prior to the first addition of Fe(II) was used as spectral reference. 100 μM Fe(II) was added to anaerobic complexes of KDM4E:2OG in the presence of substrate (H3K9me3, H3K9me2, H3K9me1 or H3K9me0, 2.0 mM) to form KDM4E:2OG:Fe(II):substrate complexes.

Stopped-flow UV-visible Absorption Spectroscopic Experiments

Deoxygenated solutions of 1 mM KDM4E, 10 mM 2OG, 0.9 mM Fe(II) and the corresponding peptide (5 mM) were prepared in 50 mM Hepes/500 mM NaCl, pH 7.5, and mixed in an anaerobic glove box. The resulting solution was rapidly mixed at 5 °C in a 1:1 ratio with a buffered solution that had been saturated with oxygen. Subsequent analysis used an SX20 stopped-flow spectrometer (Applied Photophysics, Leatherhead, UK) and spectra were recorded over time up to 1000 s, corrected for absorbance observed on mixing with anaerobic buffer. All assays were performed at least in triplicate. Analysis of kinetic data was performed using SigmaPlot™ (as described in Supplementay Figure S4).

Rapid Chemical Quench Experiments

Rapid chemical quench experiments were performed using the same conditions described above but quenching the reaction with 5% NH_4OH after defined time points post-mixing. Demethylation levels of H3K9me3 and H3K9me2 peptides were determined by MALDI-MS: Recrystallized α-cyano-4-hydroxycinnamic acid MALDI matrix (1 μL) and the quenched assay mix (1 μL) (diluted with 20 mM ammonium citrate dibasic to 10 μM peptide) were spotted onto a MALDI sample plate, and analyzed using a Waters Micromass™ MALDI microMX™ mass spectrometer, as described above. Succinate production was measured using Liquid Chromatography-Mass Spectrometry Analysis (LC-MS): Chromatographic separation was performed at 25 °C using an ACE C_{18}-

pentafluorophenyl (PFP) column (2.1 × 250 mm) on a Waters ACQUITYTM ultra-performance liquid chromatography (UPLC) system (Waters Corp., Milford, MA, USA). The following eluents were used: mobile phase A H_2O, 0.2% HCO_2H (v/v); mobile phase B MeOH, 0.2% HCO_2H (v/v). The elution gradient was 0 – 1.0 min isocratic 5% B, 1.0 – 5.0 min linear from 5% to 90% B, 5.0 – 8.0 min isocratic 90% B, and 8.0 – 9.0 min linear from 90% to 5% B, with 9.0 – 10.0 min at 5% B for re-equilibration of the column. A constant flow rate of 0.2 mL/min was used. Analytes were detected on an electrospray ionization (ESI) time-of-flight (TOF) mass analyser (Waters Corp., Manchester, UK) using a cone voltage of 60 V and a capillary voltage of 3.0 kV in negative ionisation mode. The desolvation temperature was set to 190 °C and the source temperature to 100 °C. 2OG and succinate concentrations were determined by comparison with an external calibration curve. In order to determine apparent first order rate constants of product formation, data were fitted using the equation f=y0+a*(1-exp(-b*x)) using SigmaPlot™.

RESULTS AND DISCUSSION

Variation of KDM4E activity with O_2 availability

To investigate the sensitivity of KDM4E to variations in O_2 concentration, steady-state assays were conducted with ARKme3STGGK (H3K9me3) and ARKme2STGGK (H3K9me2) peptide fragments (H3 Ala7 to Lys14, N^{ε}-methylated at residue Lys9) in a hypoxic chamber at 37 °C where the partial pressure of O_2 was varied from 0.5 to 20.6% (Figure 2). Although comparisons between *in vitro* and physiological O_2 levels cannot easily be made, under the conditions studied, KDM4E shows a near linear response to variations in O_2 concentration. (The saturating concentrations of O_2 for KDM4E appear be above the concentration of atmospheric O_2, therefore it was not possible to determine K_M for O_2 under the assay conditions.) This observation reveals the potential for histone demethylases to demonstrate a graded response to changes in O_2 availability. Further studies were therefore conducted to investigate the kinetics of the reaction of KDM4E with O_2.

Steady-state KDM4E assay at 5 °C

Previous studies on KDM4 demethylases catalysis were carried out at room temperature or above [12,14]. Knowing that enzymatic activity is usually temperature-dependent, we measured the steady-state kinetics for KDM4E at 5 °C (for comparison with pre-steady state assays) using a matrix-assisted laser desorption/ionization mass spectrometry (MALDI-MS) method [12] (Table 1 and Supplementary Figure S2). The K_M value for the H3K9me3 8mer peptide fragment was similar to the K_M value obtained for the H3K9me2 peptide (14.0 μM and 18.2 μM, respectively). Likewise, both peptides showed similar k_{cat} values (0.048 s^{-1} for the H3K9me3 peptide and 0.040 s^{-1} for the H3K9me2 peptide). This may indicate that the binding affinities of the H3K9me3 and H3K9me2 peptides are not limiting for KDM4E catalysis under steady-state conditions. The relative k_{cat} and K_M values for the two substrates at 5 °C are similar to those reported previously using a HCHO release assay conducted at 37 °C [13] (Table 1). Larger differences between the K_M values at 5 °C and those obtained by NMR [15] at 25 °C (203 μM for the H3K9me3 peptide and 282 μM for the H3K9me2 peptide) may reflect differences in buffer conditions affecting enzyme activity or O_2 availability (Table 1).

UV-visible absorption spectroscopic studies of the enzyme complex under anoxic conditions

We then carried out UV-visible spectroscopic studies of KDM4E:Fe(II):2OG complex formation in the absence and presence of the H3K9 peptide substrates with different methylation states (me3/me2/me1/me0), to investigate similarities with other Fe(II)/2OG oxygenases and the influence of methylation state on the enzyme-substrate complex formation. Fe(II) was titrated into a solution containing KDM4E and 2OG (Supplementary Figure S3), leading to formation of a KDM4E:2OG:Fe(II) complex with λ_{max} at ~540nm (Figure 3). As with previous studies on other 2OG oxygenases [16], this feature can be attributed to metal chelation by the 2OG C-1 carboxylate and C-2 carbonyl groups, as predicted by crystallisation studies [13]. Upon addition of H3K9me3 peptide, a shift in the λ_{max} of the absorption feature to 532nm occurs (Figure 3), consistent with a shift from a 6- to a 5-coordinate Fe, also observed for other 2OG oxygenases, and proposed to facilitate O_2 binding [17,18]. With H3K9me1 and H3K9me0 peptides, a shift in the λ_{max} to ~530nm was also observed (Figure 3), despite these peptides being poor or unproductive substrates, respectively (see below) [19]. With the H3K9me2 peptide, which is a good substrate (Figure 3, Table 1) [15], we did not observe a clear shift in the λ_{max} to ~530nm, but observed peak broadening (Figure 3). These results are consistent with spectroscopic features observed with other 2OG oxygenases, indicating the formation of homologous enzyme.Fe(II). 2OG.substrate complexes prior to oxygen binding. It is possible that the differences observed in the absorption spectra for H3K9me2 *vs.* H3K9me3/me1 reflect differences in active site binding chemistry. Crystallographic studies of the closely related histone demethylase KDM4A reveal that the N^{ε}-methyl group binding pocket is adjacent to the Fe(II), and that the me3, me2 and me1 methylation states can bind differently [20] (Supplementary Figure S1). Although structural data for KDM4E in the presence of substrates are not available, the homology between KDM4E and KDM4A suggests that the H3K9 substrates bind similarly. Interestingly for the H3K9me2 substrate, two conformations of the dimethyllysine are observed (Supplementary Figure S1), suggesting a degree of flexibility in H3K9me2 substrate binding, which may be reflected in the spectroscopic differences with H3K9me3 binding.

Stopped-flow absorption spectroscopic studies of the reaction of the enzyme complex with oxygen

To investigate the rate of reaction of KDM4E:Fe(II):2OG:H3K9 peptide substrates with O_2, and thus compare the rate of this reaction with analogous reactions of other 2OG oxygenases, stopped-flow UV-vis spectroscopy experiments were employed. An anaerobic solution of KDM4E, 2OG, Fe(II) and H3K9me3 8mer peptide was rapidly mixed (1:1) with O_2-saturated buffer at 5 °C to initiate the reaction by O_2 binding. On reaction with O_2, a new feature at 320nm is apparent (Figure 4A), as with other studied 2OG oxygenases, which was previously attributed to a high-spin Fe(IV)-oxo intermediate (V, Figure 1)[6-8]. The stopped-flow 320 nm absorbance traces were fitted to a 4-step kinetic model to obtain apparent first order rate constants of its transient formation and decay (Supplementary Figure S4). Maximum accumulation (t_{max}) of the 320 nm species occurs at 11 s (apparent formation and decay rate constants, 0.1 s^{-1} and 0.042 s^{-1}, respectively, Table 2 and

Supplementary Figure S4(a)), which is more rapid than that observed for PHD2 (t_{max} = 200 s; 0.06 s^{-1} and 0.001 s^{-1}, respectively [8]), but slower than for TauD (t_{max} = 20 - 25 ms; 42 s^{-1} and 13 s^{-1}, respectively [7]), and PBCV-vCPH (t_{max} = < 10 ms; formation and decay rate constants not determined [6]). In the absence of substrate, mixing with oxygenated buffer results in slower formation of the 320nm species (t_{max} = 78 s, Figure 4A, Table 2, Supplementary Figure S4(d)), consistent with the known ability of 2OG oxygenases to catalyze 2OG turnover in the absence of their prime substrate, and demonstrating the ability of H3K9me3 to enhance the rate of reaction with O_2. The spectroscopic shift from 6C- to 5C- Fe(II) coordination state observed in the KDM4E:Fe(II):2OG:H3K9me3 complex formation studies is in a good agreement with the faster reaction of KDM4E in the presence of peptide substrate as “substrate triggering” is one of defining characteristics of O_2-activating enzymes and reflects the facilitation of O_2-binding in the presence of a prime substrate.

The substrate affinity of KDM4E can increase with peptide length [there is a substantial drop in K_M with increased substrate length (from 21.3 μM for the 8mer H3K9me3 peptide to 0.8 μM for the 25mer H3K9me3 peptide)] affecting rates of individual steps of the catalytic pathway if substrate binding or product release is limiting [19]. Therefore, to exclude the possibility of sluggish reaction of KDM4E with O_2 due to sub-optimal substrate binding, stopped-flow UV-vis spectroscopy was carried out in the presence of the H3K9me3 25mer. Development of the 320nm species was not faster for the 25mer peptide (t_{max} = 11 s, Figure 4B, Supplementary Figure S4(b)) than for the 8mer H3K9me3 peptide, and similar apparent formation and decay rate constants were obtained (Table 2), indicating that the rate of 320nm species formation is not limited by inefficient substrate binding.

In order to study the influence of histone methylation state on the rate of the reaction of KDM4E with O_2, we then carried out stopped-flow UV-vis spectroscopy in the presence of the H3K9me2 peptide. Interestingly, formation of the 320nm species was slower in the presence of H3K9me2 than H3K9me3 (t_{max} = 24 s *vs.* 11 s, respectively; Figure 4C, Supplementary Figure S4(c)), though comparable rates of degradation were observed (Table 2). Although mechanistic conclusions cannot be drawn without characterisation of the species absorbing at 320nm, these results suggest that at least one aspect of KDM4E catalysis is slower in the presence of the H3K9me3 peptide than the H3K9me2 peptide.

Interestingly, we also observed that development of the absorption at 320nm was significantly slower in the presence of H3K9me1 (t_{max} = 46 s, Supplementary Figures S4(e) and S5) and H3K9me0 peptides (t_{max} = 72 s, Supplementary Figures S4(f) and S5). Indeed, with the H3K9me0 peptide the apparent rate constants of formation and decay are similar to those obtained in the absence of any substrate (Table 2) indicating that in this case the observed absorbance features may represent uncoupled 2OG oxidation. Stopped-flow 320nm absorbance traces for these unproductive reactions were fitted to a 2-step kinetic model (Supplementary Figure S4). It has previously been demonstrated that KDM4E is unable to demethylate an H3K9me1 8mer peptide within limits of detection, proposed to be due to inefficient binding of the methyl group in the correct orientation (Supplementary Figure S1) [13,15]. The slower formation and degradation of the 320nm species in the presence of H3K9me1/H3K9me0 peptides may be due to this unproductive binding.

Rapid chemical quench studies of the reaction of the enzyme complex with oxygen

To investigate whether the kinetics of formation and decay of the 320nm-absorbing species correspond with events on the catalytic pathway, rapid chemical quench experiments (coupled to mass-spectrometric analyses) were conducted under the same conditions used for the stopped-flow UV-visible experiments (Figure 5). In the presence of H3K9me3 substrate, demethylation occurred with a rate constant of 0.014 s^{-1} and succinate production with a similar rate constant of 0.011 s^{-1}. These similar rates are consistent with the tightly coupled 2OG turnover and H3K9me3 demethylation observed for KDM4E [15] under steady-state conditions. Coupled turnover was also observed in this study by NMR spectroscopy under similar conditions to those used in the rapid-quench flow experiments (Supplementary Figure S7). Tight coupling of 2OG oxidation and histone demethylation is important for effective functioning of the enzyme in cells preventing accumulation of succinate and possible enzyme inactivation if uncoupled turnover proceeds via a different mechanism [5]. In the presence of the H3K9me3 substrate, di- and monomethylated peptide products were observed at a ratio of approximately 5:1, respectively, after 15 min at 5 °C (Supplementary Figure S7), indicating that under the conditions used, the kinetics predominantly represent the turnover of H3K9me3 to H3K9me2. Demethylation of the H3K9me2 substrate to the monomethylated peptide product occurred at a similar rate, 0.02 s^{-1}, to that observed for H3K9me3 (Supplementary Figure S8). Although demethylation begins at approximately t_{max} for the 320nm species, the rates of demethylation/succinate production (0.014 s^{-1}/0.011 s^{-1}) are slower than the rates of degradation of the 320nm species for H3K9me3 substrate (Table 2). This is consistent with the observed 320nm species representing a catalytic intermediate that occurs prior to demethylation. These results again indicate a slow reaction of KDM4E with O_2; interestingly, the apparent rate constant of demethylation of H3K9me3 by KDM4E upon mixing with O_2 is comparable to that observed for HIF hydroxylation by the O_2 sensor PHD2 under similar conditions (0.014 s^{-1} and 0.013 s^{-1}, respectively) [8].

Overall the results support the proposal that the mechanism of 2OG-dependent KDMs proceed in a similar sequence to the 2OG oxygenases [6,7,17]. Notably, the results also reveal that the rate of reaction of the enzyme:Fe(II):2OG:substrate complex with O_2 is relatively slow, as observed for PHD2 [8], at least compared to the other studied 2OG oxygenases [6,7,17,18]. As discussed above it is possible that this property is characteristic of an O_2 sensing oxygenase [8]. In a cellular context, factors other than O_2 activity can regulate oxygenase catalysis. Nonetheless the results with KDM4E are supportive of the proposal that KDM catalysis may, in some circumstances, be regulated by O_2 availability.

Supplementary Material

Refer to Web version on PubMed Central for supplementary material.

Acknowledgments

FUNDING

The research leading to these results has received funding from the *European Union* Seventh Framework Programme *(FP7/2007-2013)* under *grant agreement* n° [252217] (EMSF). This work is also supported by a

Clarendon-St. Hugh' s College-Louey Scholarship (HT), King Faisal Specialist Hospital and Research Center, Riyadh 11211, Saudi Arabia (KAQ), the Wellcome Trust and the BBSRC (RJH), the European Research Council (CJS) and a Royal Society Dorothy Hodgkin Fellowship (EF).

Abbreviations used

2OG	2-oxoglutarate
Jmj	Jumonji
H3K9	histone H3 lysine9
KDM	histone-lysine demethylase
SI	Supplementary Information
TauD	taurine dioxygenase
vCPH	viral prolyl-4-hydroxylase
PHD2	prolyl hydroxylase 2
HIF	hypoxia-inducible factor
MALDI-MS	matrix-assisted laser desorption/ionization mass spectrometry
CHCA	α-cyano-4-hydroxycinnamic acid
LC-MS	liquid chromatography-mass spectrometry analysis
t_{max}	maximum accumulation

REFERENCES

1. Ng SS, Yue WW, Oppermann U, Klose RJ. Dynamic protein methylation in chromatin biology. Cell Mol. Life Sci. 2009; 66:407–422. [PubMed: 18923809]
2. Shi Y. Histone lysine demethylases: emerging roles in development, physiology and disease. Nat. Rev. Genet. 2007; 8(11):829–833. [PubMed: 17909537]
3. Klose RJ, Zhang Y. Regulation of histone methylation by demethylimination and demethylation. Nat. Rev. Mol. Cell Biol. 2007; 8(4):307–318. [PubMed: 17342184]
4. Schofield CJ, Zhang ZZ. Structural and mechanistic studies on 2-oxoglutarate-dependent oxygenases and related enzymes. Curr. Opin. Struct. Biol. 1999; 9(6):722–731. [PubMed: 10607676]
5. Hausinger RP. Fe(II)/α-Ketoglutarate-Dependent Hydroxylases and Related Enzymes. Crit. Rev. Biochem. Mol. 2004; 39(1):21–68.
6. Hoffart LM, Barr EW, Guyer RB, Bollinger JM Jr. Krebs C. Direct spectroscopic detection of a C-H-cleaving high-spin Fe(IV) complex in a prolyl-4-hydroxylase. Proc. Natl. Acad. Sci. U.S.A. 2006; 103(40):14738–14743. [PubMed: 17003127]
7. Price JC, Barr EW, Tirupati B, Bollinger JM Jr. Krebs C. The First Direct Characterization of a High-Valent Iron Intermediate in the Reaction of an α-Ketoglutarate-Dependent Dioxygenase: A High-Spin Fe(IV) Complex in Taurine/α-Ketoglutarate Dioxygenase (TauD) from Escherichia coli. Biochemistry. 2003; 42(24):7497–7508. [PubMed: 12809506]
8. Flashman E, Hoffart LM, Hamed RB, Bollinger JM Jr. Krebs C, Schofield CJ. Evidence for the slow reaction of hypoxia-inducible factor prolyl hydroxylase 2 with oxygen. Febs J. 2010; 277(19): 4089–4099. [PubMed: 20840591]
9. Watson JA, Watson CJ, McCann A, Baugh J. Epigenetics, the epicenter of the hypoxic response. Epigenetics. 2010; 5:293–296. [PubMed: 20418669]

10. Tausendschön M, Dehne N, Brüne B. Hypoxia causes epigenetic gene regulation in macrophages by attenuating Jumonji histone demethylase activity. Cytokine. 2011; 53:256–262. [PubMed: 21131212]
11. Pollard PJ, Loenarz C, Mole DR, McDonough MA, Gleadle JM, Schofield CJ, Ratcliffe PJ. Regulation of Jumonji-domain-containing histone demethylases by hypoxia-inducible factor (HIF)-1α. Biochem. J. 2008; 416(3):387–394. [PubMed: 18713068]
12. Katoh M, Katoh M. Identification and characterization of JMJD2 family genes in silico. Int. J. Oncol. 2004; 24(6):1623–1628. [PubMed: 15138608]
13. Hillringhaus L, Yue WW, Rose NR, Ng SS, Gileadi C, Loenarz C, Bello SH, Bray JE, Schofield CJ, Oppermann U. Structural and Evolutionary Basis for the Dual Substrate Selectivity of Human KDM4 Histone Demethylase Family. J. Biol. Chem. 2011; 286(48):41616–41625. [PubMed: 21914792]
14. Rose NR, Ng SS, Mecinovic J, Lienard BM, Bello SH, Sun Z, McDonough MA, Oppermann U, Schofield CJ. Inhibitor Scaffolds for 2-Oxoglutarate-Dependent Histone Lysine Demethylases. J. Med. Chem. 2008; 51(22):7053–7056. [PubMed: 18942826]
15. Hopkinson RJ, Hamed RB, Rose NR, Claridge TD, Schofield CJ. Monitoring the Activity of 2-Oxoglutarate Dependent Histone Demethylases by NMR Spectroscopy: Direct Observation of Formaldehyde. ChemBioChem. 2010; 11(4):506–510. [PubMed: 20095001]
16. Zhou J, Kelly WL, Bachmann BO, Gunisor M, Townsend CA, Solomon EI. Spectroscopic Studies of Substrate Interactions with Clavaminate Synthase 2, a Multifunctional α-KG-Dependent Non-Heme Iron Enzyme: Correlation with Mechanisms and Reactivities. J. Am. Chem. Soc. 2001; 123:7388–7398. [PubMed: 11472170]
17. Price JC, Barr EW, Hoffart LM, Krebs C, Bollinger JM Jr. Kinetic Dissection of the Catalytic Mechanism of Taurine: α-Ketoglutarate Dioxygenase (TauD) from Escherichia coli. Biochemistry. 2005; 44(22):8138–8147. [PubMed: 15924433]
18. Ryle MJ, Padmakumar R, Hausinger RP. Stopped-Flow Kinetic Analysis of Escherichia coli Taurine/α-Ketoglutarate Dioxygenase: Interactions with a-Ketoglutarate, Taurine, and Oxygen. Biochemistry. 1999; 38(46):15278–15286. [PubMed: 10563813]
19. Rose, NR. Structural, Mechanistic and Inhibition Studies on the Histone Lysine Demethylases. University of Oxford; 2009. Chemistry Department
20. Ng SS, Kavanagh KL, McDonough MA, Butler D, Pilka ES, Lienard BM, Bray JE, Savitsky P, Gileadi O, von Delft F, Rose NR, Offer J, Scheinost JC, Borowski T, Sundstrom M, Schofield CJ, Oppermann U. Crystal structures of histone demethylase JMJD2A reveal basis for substrate specificity. Nature. 2007; 448(7149):87–91. [PubMed: 17589501]

Europe PMC Funders Author Manuscripts

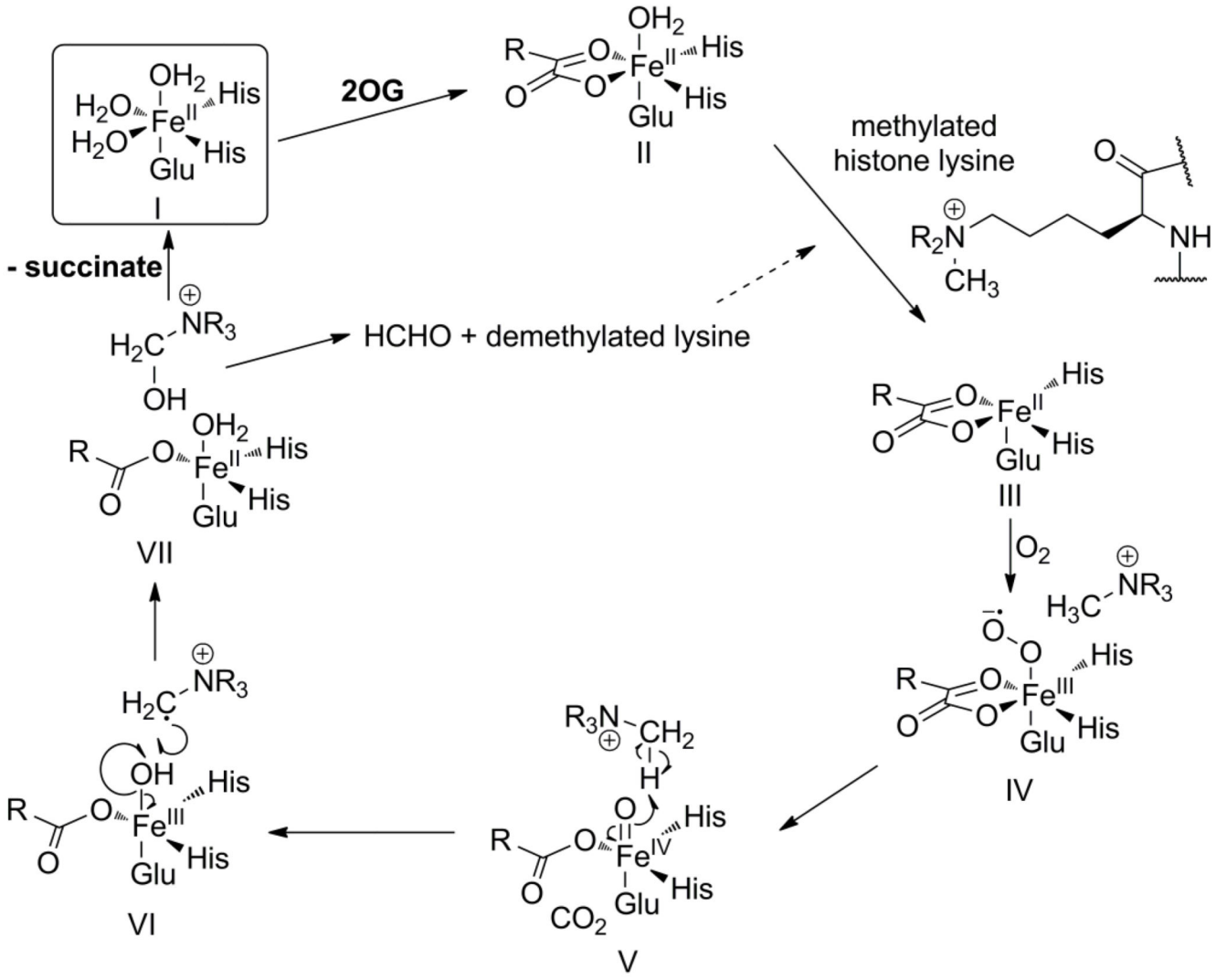

Figure 1. Proposed mechanism of KDM4E

Proposed mechanism of KDM4E based on the consensus mechanism for the 2OG oxygenases: O_2 is the final substrate to bind to the KDM4E:Fe(II):2OG:H3K9 complex (**I-III**) resulting in generation of a Fe(IV)-oxo species that enables hydroxylation of the unactivated C-H bond (**IV-VI**). The unstable hydroxymethyl product is released as HCHO (**VII**), to give the *N*-demethylated product [5,6].]

Europe PMC Funders Author Manuscripts

Europe PMC Funders Author Manuscripts

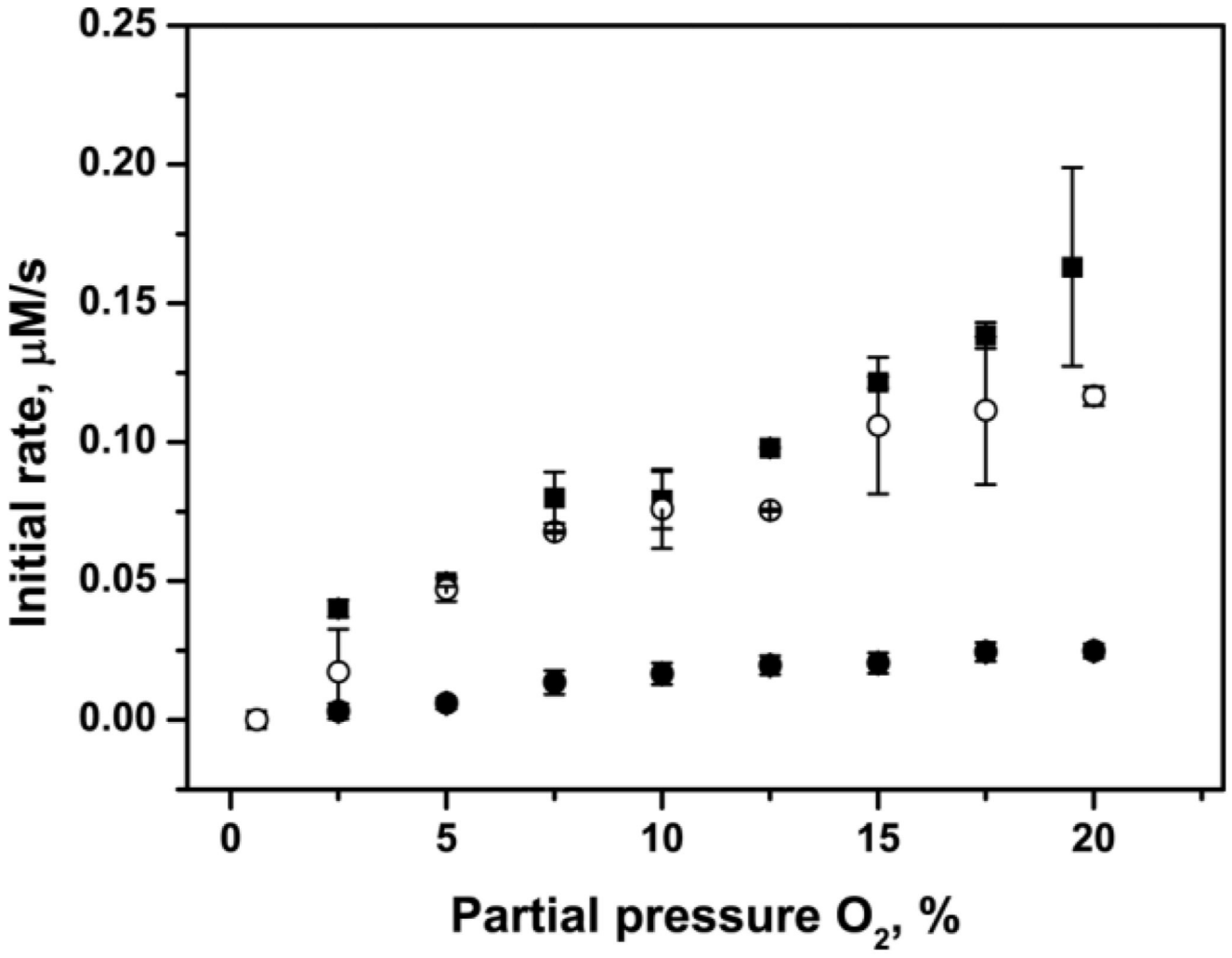

Figure 2. Variation of KDM4E activity with O_2 availability

MALDI-MS was used to determine conversion at 37 °C of H3K9me3 to both H3K9me2 (black squares) and H3K9me1 (black circles), and separately, conversion of H3K9me2 to H3K9me1 (white circles).

Europe PMC Funders Author Manuscripts

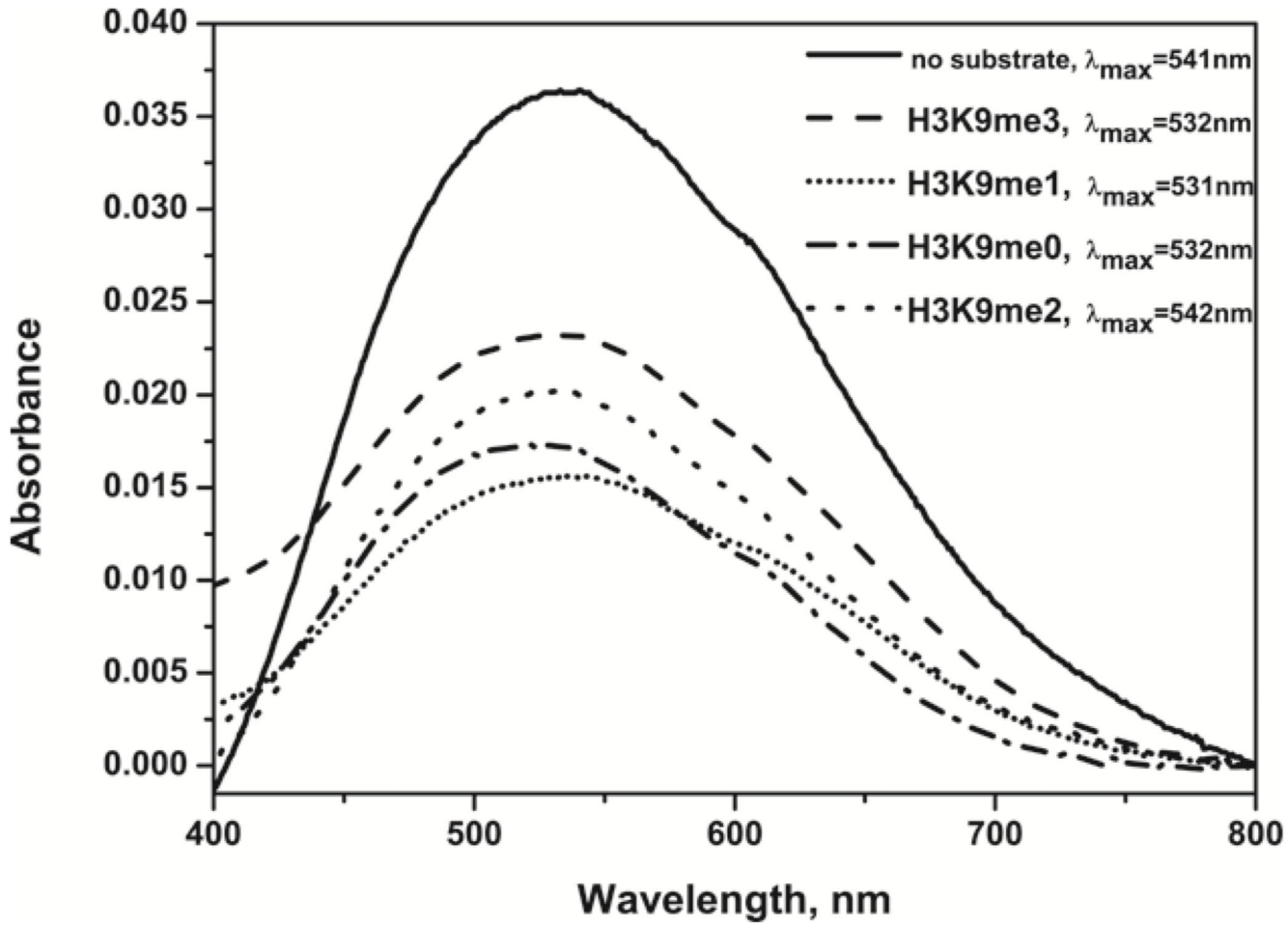

Figure 3. UV-visible Absorption Spectroscopy

Absorption spectra of anaerobic KDM4E:Fe(II):2OG and KDM4E:Fe(II):2OG:H3K9 complexes at room temperature (KDM4E:2OG absorbance subtracted). KDM4E, 0.4 mM; 2OG, 4 mM; H3K9 peptides, 2 mM; Fe(II), 100 μM.

Europe PMC Funders Author Manuscripts

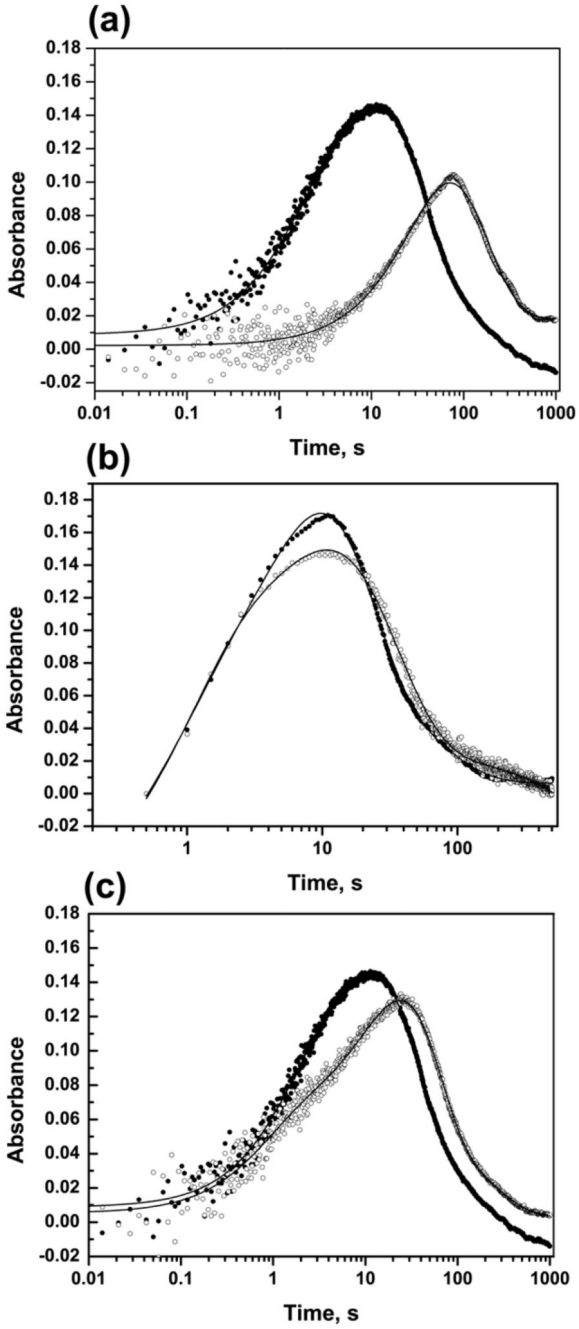

Figure 4. Stopped-flow UV-visible Absorption Spectroscopy

(**a**) UV-Vis absorbance spectra at 320nm from stopped-flow experiments mixing KDM4E:Fe(II):2OG:H3K9me3 8mer (black) or KDM4E:Fe(II):2OG (white) with O_2. (**b**) UV-Vis absorbance spectra at 320nm from stopped-flow experiments mixing KDM4E:Fe(II):2OG:H3K9me3 8mer (black) or KDM4E:Fe(II):2OG:H3K9me3 25mer (white) with O_2. (**c**) UV-Vis absorbance spectra at 320nm from stopped-flow experiments mixing KDM4E:Fe(II):2OG: H3K9me3 8mer (black) or KDM4E:Fe(II):2OG:H3K9me2 8mer (white) with O_2. Concentrations before mixing: KDM4E (1.0 mM), Fe(II) (900 μM),

2OG (10 mM), peptide (5 mM) and O_2 (1.9 mM). Reactions were carried out at 5 °C. Spectra were recorded over 0.001-1000 s, corrected for absorbance observed on mixing with anaerobic buffer.

Europe PMC Funders Author Manuscripts

Europe PMC Funders Author Manuscripts

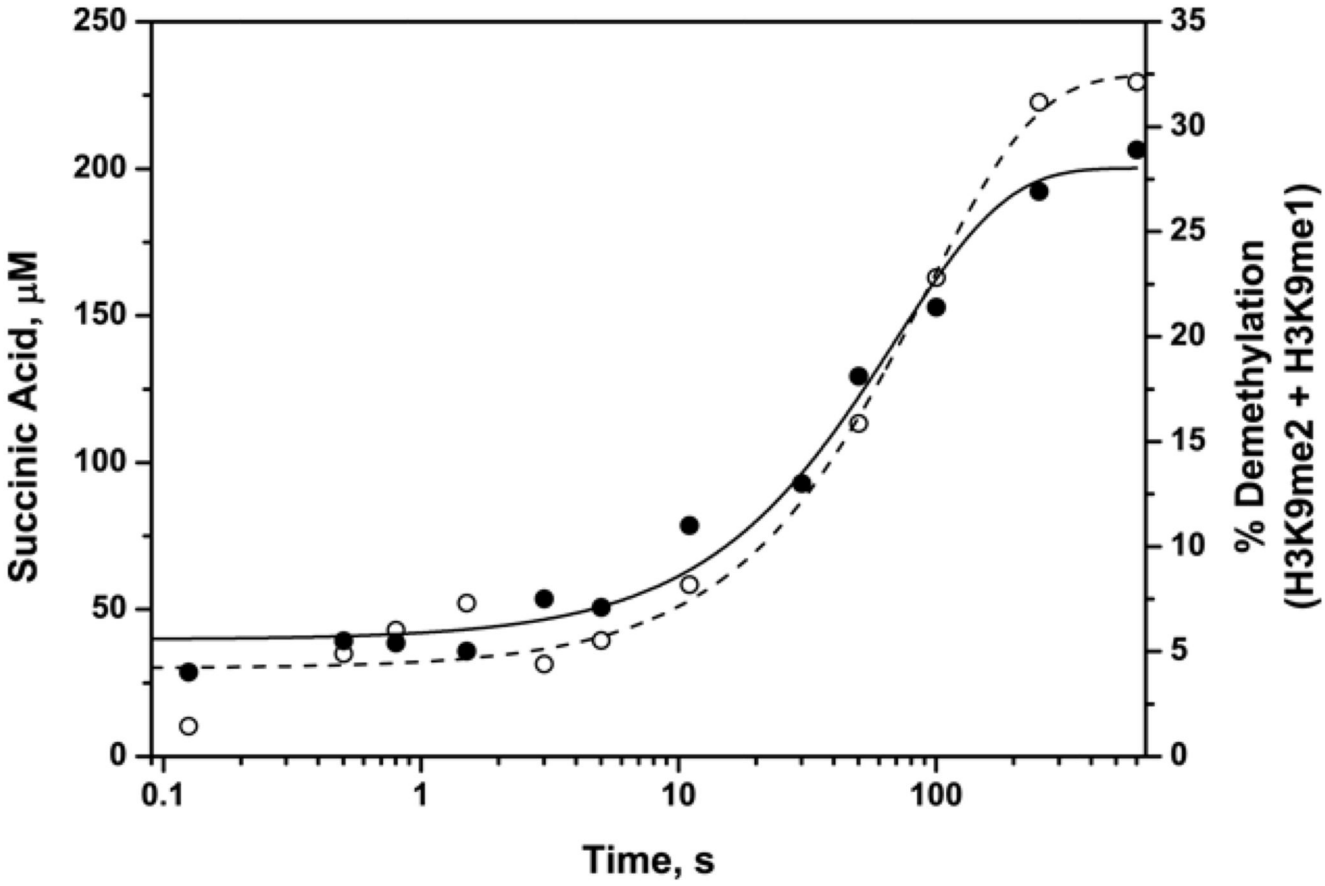

Figure 5. Rapid chemical quench in the presence of H3K9me3 8mer peptide

Rapid chemical quench experiments for H3K9me3 8mer peptide revealed that demethylation occurred at 0.014 s^{-1} (black) and 2OG decarboxylation to succinate (white) at 0.011 s^{-1} (shown on a logarithmic scale), as determined by MALDI-MS and LC-MS, respectively. (In both cases data were fitted with the equation f = y0+a*(1-exp(-b*x)), using SigmaPlot™). Concentrations before mixing were KDM4E (1.0 mM), Fe(II) (900 μM), 2OG (10 mM), peptide (5 mM) and O_2 (1.9 mM). Reactions were carried out at 5 °C.

Europe PMC Funders Author Manuscripts

Table 1

Steady-state kinetic parameters for KDM4E determined under different experimental conditions

	k_{cat} (s^{-1})		K_M (μM)	
Assay	**H3K9me3**	**H3K9me2**	**H3K9me3**	**H3K9me2**
MALDI-MS (5°C)	0.048 ± 0.001	0.040 ± 0.001	14.0 ± 1.9	18.2 ± 3
NMR (25 °C)	0.018 ± 0.002	0.02 ± 0.001	203 ± 79	282 ± 36
HCHO release (37°C)	0.076 ± 0.01	0.065 ± 0.002	23 ± 4	25 ± 3

Substrates were 8mer peptides. Mean values and standard deviations for k_{Cat} and K_M (n = 3) are shown.

Europe PMC Funders Author Manuscripts

Table 2

Kinetic parameters for the 320nm species from stopped-flow experiments observed upon mixing KDM4E:Fe(II):2OG ± H3K9 peptides with O_2

	t_{max} (s)	Formation rate constant (s^{-1})	Decay rate constant (s^{-1})
No substrate	78	0.025 ± 0.0008	0.008 ± 0.0003
H3K9me3	11	0.1 ± 0.007	0.042 ± 0.003
H3K9me3 25mer	11	0.09 ± 0.009	0.053 ± 0.004
H3K9me2	24	0.050 ± 0.006	0.030 ± 0.004
H3K9me1	46	0.032 ± 0.0003	0.014 ± 0.0001
H3K9me0	72	0.019 ± 0.0002	0.009 ± 0.0001

Standard errors are shown.